Supplementary Methods

Antibody Characterization

The mouse anti-PV antibody (Cat#235, Lot#10-11F, Swant) recognized a single band at the expected size of 12 kDa by western blotting and showed an absence of immunoreactivity by immunohistochemistry in PV knockout mice[1,2]. The goat anti-CR antibody (Cat#CG1, Lot#1ξ1, Swant) showed an absence of immunoreactivity by immunohistochemistry in CR knock-out mice[3]. The guinea pig anti-VGlut1 antibody (Cat#AB5905, Lot#22430498, Millipore) recognized a single band at the expected size of 60 kDa by western blotting[4] and preadsorption with the immunogen peptide abolished immunolabeling (reported by the manufacturer). The rabbit anti-PSD-95 antibody (Cat#3450s, Lot#2, Cell Signaling) recognized a single band of 95 kDa on western blots from extracts of rat brain and human cerebellum as reported by the manufacturer, and highly co-localized with immunolabeling of a well-characterized mouse monoclonal anti-PSD-95 antibody (Neuromab cat. no. 75-028)[5]. All secondary and tertiary antibodies used in this study were shown to produce minimum cross-reactivity by the manufacturers.

PMI effect on protein immunoreactivity

Because PMI may affect protein immunoreactivity[6], we assessed the density of VGlut1+/PSD95+ puncta onto PV+ cell bodies in 6 control subjects with PMIs ranging from 4.8 to 22.7 hours. The density of Vglut1+/PSD95+ puncta onto PV+ cell bodies was not correlated with PMI in these subjects ($R=-0.111$, $p=0.835$), suggesting that the detectability of excitatory inputs is not influenced by a PMI less than 24 hours.

Antibody Penetration Efficiency Analysis

To check for penetration efficiency of anti-VGlut1 or anti-PSD95 antibody, we preliminarily assessed the distribution of VGlut1+ or PSD95+ masks along the Z-axis in ten random image stacks from control subjects. Z-axis per each image was divided into 10 bins, with each bin representing the 10% of total Z-axis from the top (100%) to the bottom (1%) of the section. Mean percent localization of VGlut1+ or PSD95+ masks in 1~10% and 91~100% of the Z-axis were significantly different from those in the middle 80% of the Z-axis (VGlut1: $F_{9,90}=9.5, p<0.001$; PSD95: $F_{9,90}=20.9, p<0.001$; post hoc tukey's test $p<0.05$). Therefore, only the objects localized within the 80% of middle z-planes (~32 μm) were sampled for data analysis.

VGlut+ and PSD95+ puncta segmentation

First, a custom channel was made for each deconvolved channel of VGlut1 or PSD95 by calculating a difference of Gaussians using sigma values of 0.7 and 2. Then, the Ridler-Calvard threshold value was applied to the fluorescence intensity histogram of either VGlut1+ or PSD95+ labeling and all pixels were reassigned to a binary value according to whether they were above or below the threshold value, and the resulting binary image was referred to as the object mask. Then these object masks were automatically defined as VGlut1+ or PSD95+ masks if they fell in the range of defined puncta size (0.06-0.7μm^3)[7]. Choosing a single threshold value may not be sufficient to ensure comprehensive masking of VGlut1+ and PSD95+ puncta, as protein levels differ within synaptic structures and vary substantially as a result of disease states. Therefore, we utilized the MATLAB script, which performs multiple iterations of automated masking process that starts from the Ridler-Calvard threshold value and incrementally migrates towards the highest intensity value. The resulting object masks from each iteration were combined to represent the total population of VGlut1+ or PSD95+ puncta. Lipofuscin autofluorescence labeling was masked using the Ridler-Calvard threshold value as explained above and was subtracted from the VGlut1+ or PSD95+ masks for final analysis.

Supplement references

1. Celio MR, Baier W, Scharer L, de Viragh PA, Gerday C. Monoclonal antibodies directed against the calcium binding protein parvalbumin. *Cell calcium.* 1988;9(2):81-86.
2. Schwaller B, Dick J, Dhoot G, et al. Prolonged contraction-relaxation cycle of fast-twitch muscles in parvalbumin knockout mice. *The American journal of physiology.* 1999;276(2 Pt 1):C395-403.
3. Schiffmann SN, Cheron G, Lohof A, et al. Impaired motor coordination and Purkinje cell excitability in mice lacking calretinin. *Proc Natl Acad Sci U S A.* 1999;96(9):5257-5262.
4. Melone M, Burette A, Weinberg RJ. Light microscopic identification and immunocytochemical characterization of glutamatergic synapses in brain sections. *J Comp Neurol.* 2005;492(4):495-509.
5. Soiza-Reilly M, Commons KG. Quantitative analysis of glutamatergic innervation of the mouse dorsal raphe nucleus using array tomography. *J Comp Neurol.* 2011;519(18):3802-3814.
6. Lewis DA. The human brain revisited: opportunities and challenges in postmortem studies of psychiatric disorders. *Neuropsychopharmacology.* 2002;26(2):143-154.
7. Fish KN, Sweet RA, Deo AJ, Lewis DA. An automated segmentation methodology for quantifying immunoreactive puncta number and fluorescence intensity in tissue sections. *Brain Res.* 2008;1240:62-72.

Supplementary Table S1. Demographic, postmortem, and clinical characteristics of human subjects used in this study.

Pair #	Subject Group[a]	Case #	S/R/A[b]	PMI[c]	pH	Storage time[d]	Cause of death[e]	*DSM IV* Diagnoses[f]	Primary Substance[g]	Anti-psychotics ATOD	Anti-depressants ATOD	BZ/VPA ATOD[h]
1	C	1047	M/W/43	13.8	6.6	129	ASCVD	N				
	S	1209	M/W/35	9.1	6.5	110	Diphenhydramine overdose	SA		Y	N	N
2	C	1092	F/B/40	16.6	6.8	123	Mitral valve prolapse	N				
	S	1178	F/B/37	18.9	6.1	114	Pulmonary embolism	SA		Y	N	Y
3	C	1122	M/W/55	15.4	6.7	119	Cardiac tamponade	N				
	S	1105	M/W/53	7.9	6.2	121	ASCVD	SA		Y	N	N
4	C	1284	M/W/55	6.4	6.8	98	ASCVD	N				
	S	1188	M/W/58	7.7	6.2	113	ASCVD	US	AAR; OAR	Y	N	Y
5	C	1191	M/B/59	19.4	6.2	112	ASCVD	N				
	S	1263	M/W/62	22.7	7.1	102	Asphyxiation	US	ADR	Y	Y	N
6	C	10003	M/W/49	21.2	6.5	112	Trauma	N				
	S	1088	M/W/49	21.5	6.5	124	Combined drug overdose	US	ADC; OAC	Y	Y	N
7	C	1247	F/W/58	22.7	6.4	104	ASCVD	N				
	S	1240	F/B/50	22.9	6.3	105	ASCVD	US	ADR	Y	N	N
8	C	1099	F/W/24	9.1	6.5	122	Cardiomyopathy	N				
	S	10023	F/B/25	20.1	6.7	103	Suicide by drowning	DS		Y	Y	Y
9	C	1307	M/B/32	4.8	6.7	93	ASCVD	N				
	S	10024	M/B/37	6	6.1	103	ASCVD	PS		N	N	N
10	C	1391	F/W/51	7.8	6.6	79	ASCVD	N				
	S	1189	F/W/47	14.4	6.4	113	Combined drug overdose	SA	AAR	Y	Y	Y
11	C	1159	M/W/51	16.7	6.5	116	ASCVD	N				
	S	1296	M/W/48	7.8	6.5	96	Pneumonia	US		Y	Y	N
12	C	1326	M/W/58	16.4	6.7	90	ASCVD	N				
	S	1314	M/W/50	11	6.2	93	ASCVD	US		Y	Y	Y
13	C	1555	M/W/17	15.1	6.9	50	Trauma	N				
	S	1649	M/B/17	21.4	6.9	35	Hanging	US		Y	Y	N
14	C	1268	M/B/49	19.9	7.1	102	ASCVD	N				
	S	1230	M/W/50	16.9	6.6	108	Doxepin overdose	US		Y	Y	N
15	C	1386	M/W/46	21.2	6.7	82	ASCVD	N				
	S	1420	M/W/47	23.4	6.8	75	Jump	SA	AAR; ODC; OAR	Y	Y	N
16	C	1472	M/W/61	23.8	6.5	66	Pulmonary embolism	N				
	S	1453	M/W/62	11.1	6.4	69	Trauma	PS	ADR	Y	N	Y

17	C	694	M/W/38	20.7	7	195	Subarachnoid hemorrhage	N					
	S	1455	M/W/42	8.2	6.4	69	Peritonitis	PS	AAR; OAC	Y		N	Y
18	C	1372	M/W/37	20.5	6.6	86	Asphyxiation	N					
	S	1581	M/W/32	18.4	6.8	45	ASCVD	PS	ODC; OAC	Y		Y	N
19	C	1543	F/W/45	17.9	6.8	52	Subarachnoid hemorrhage	N					
	S	10026	F/W/46	23.8	6.6	104	Thermal injuries	US		Y		Y	N
20	C	1583	M/W/58	19.1	6.8	45	Trauma	N					
	S	1686	M/B/56	14.1	6.2	28	ASCVD	PS	AAR	Y		Y	Y

a: C, Unaffected comparison; S, schizophrenia; **b**: A, age in years; B, black; F, female; M, male; R, race; S, sex; W, white; **c**: PMI, postmortem interval (hours); **d**: Storage time (months) at -80C; **e**: ASCVD, arteriosclerotic cardiovascular disease; MCA, middle coronary artery; **f**: DS, disorganized schizophrenia; PS, paranoid schizophrenia; SA, schizoaffective disorder; US, undifferentiated schizophrenia; **g**: ADC, alcohol dependence, current at time of death; ADR, alcohol dependence, in remission at time of death; AAC, alcohol abuse, current at time of death; AAR, alcohol abuse, in remission at time of death; ODC, other substance dependence, current at time of death; ODR, other substance dependence, in remission at time of death; OAC, other substance abuse, current at time of death; OAR, other substance abuse, in remission at time of death; **h**: BZ/VPA ATOD; BZ, benzodiazepines; VPA, Sodium valproate; ATOD, at time of death; Y, yes; N, no.

Supplementary Figure legends

Supplementary Figure S1. Representative raw, deconvolved and masked images of PV+ cell bodies, CR+ cell bodies, VGlut1+ puncta, PSD95+ puncta and lipofuscin in human DLPFC. PV+ neurons with varying intensity range (white arrow – PV mean intensity: 2810 a.u., PV sum intensity: 133426234 a.u.; gray arrow – PV mean intensity: 951 a.u., PV sum intensity: 35779294 a.u.) and CR+ neurons with varying intensity range (white arrow – CR mean intensity: 3189 a.u., CR sum intensity: 50431392 a.u.; gray arrow – CR mean intensity: 1010 a.u., CR sum intensity: 7999625 a.u.) were masked as described in Methods. Lipofuscin masks (white arrowheads) were subtracted from the puncta mask for final analyses. Scale bar = 10μm.

Supplementary Figure S2. Levels of VGlut1 or PSD95 immunoreactivity within VGlut1+ puncta or PSD95+ puncta, respectively, onto PV interneurons are unaltered in schizophrenia subjects. X denotes a subject pair identified as an outlier by the Grubbs' test (Z=3.38, $p<0.01$). Statistical analyses with and without the outlier pair are shown.

Supplementary Figure S3. No effect of co-morbid factors on the mean density of VGlut1+/PSD95+ puncta onto PV+ cell bodies in subjects with schizophrenia. In each pair of plots, schizophrenia subjects are grouped by the co-morbid factors listed on the x-axis. Circles represent the levels of the mean density for individual schizophrenia subjects and the bars represent mean density for the indicated group. Numbers listed for each bar represent the number of schizophrenia subjects with that condition. Mean density of VGlut1+/PSD95+ puncta onto PV+ cell bodies in schizophrenia subjects did not differ significantly as a function of diagnosis of schizoaffective disorder, history of substance dependence or abuse, nicotine use at the time of death, use of antidepressants, or benzodiazepines and/or sodium valproate at the time of death, or death by suicide.

Supplementary Figure S4. Density of excitatory synaptic inputs to PV interneurons is not altered in monkeys treated with psychotropic medications. (**A-D**) Mean numbers of sampled PV+ neurons, mean PV immunoreactivity levels in PV+ cell bodies, mean surface area of PV+ cell bodies or mean density of VGlut1+/PSD95+ puncta onto PV+ cell bodies was not altered in the monkeys treated with haloperidol or olanzapine compared to the monkeys treated with placebo.

Supplementary Figure S1

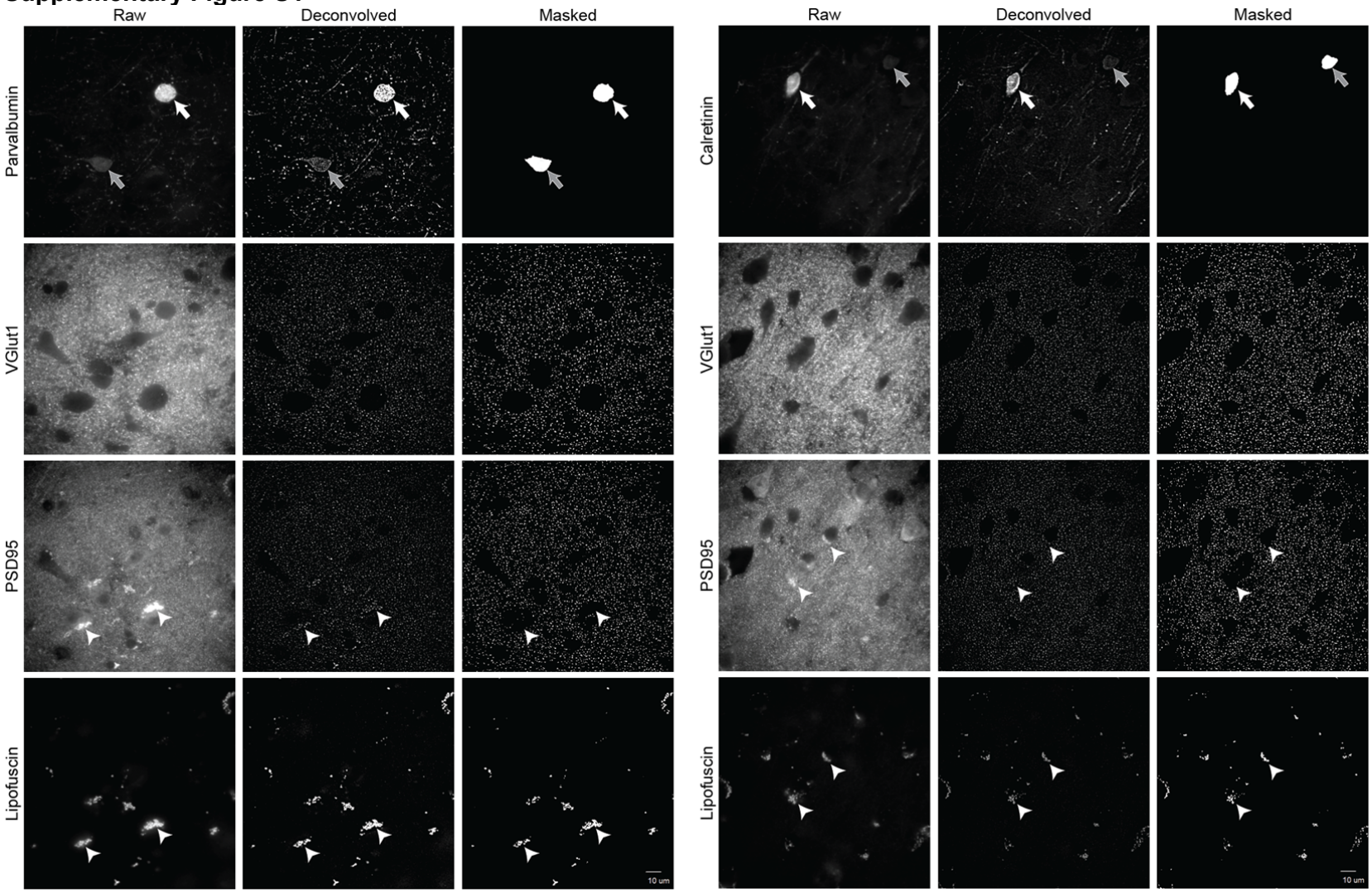

Supplementary Figure S2

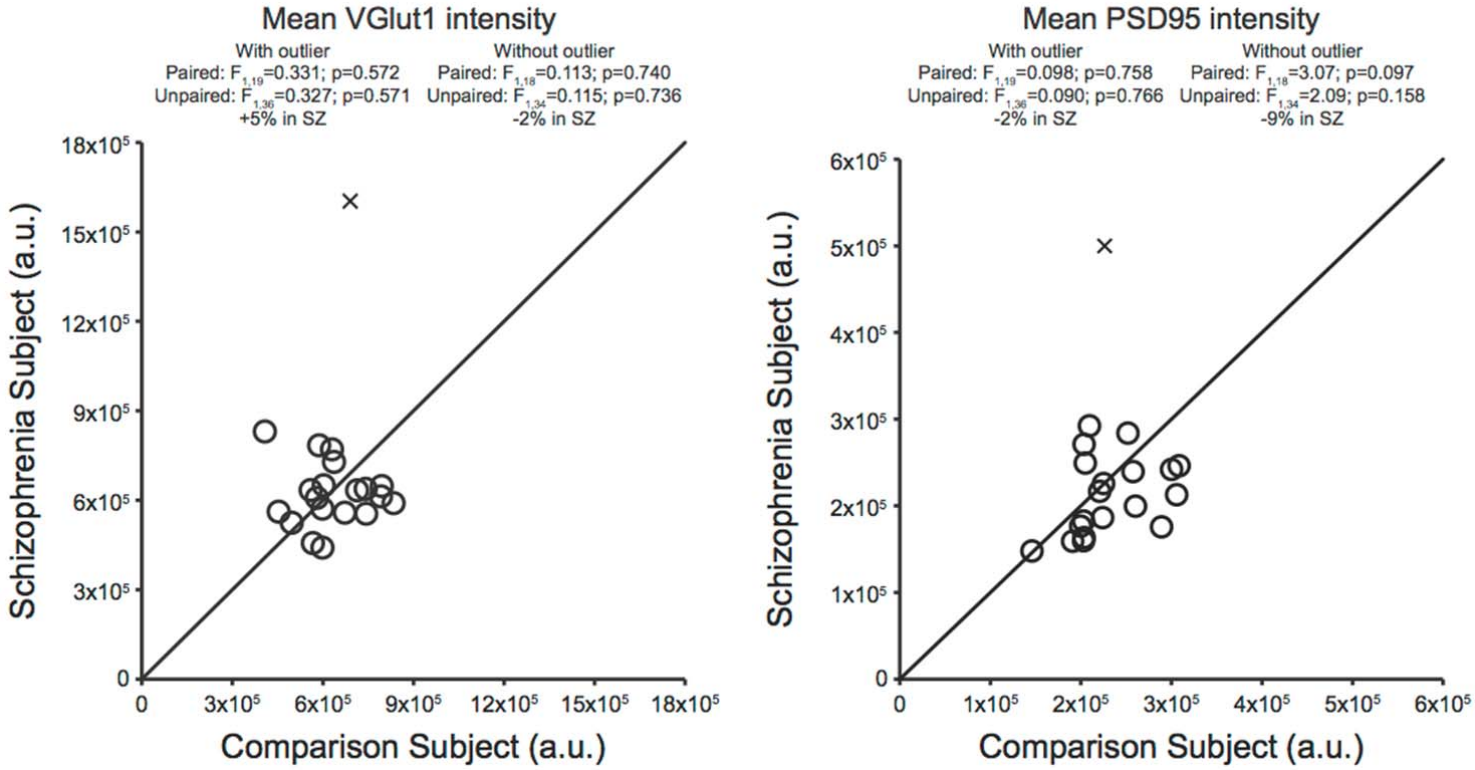

Supplementary Figure S3

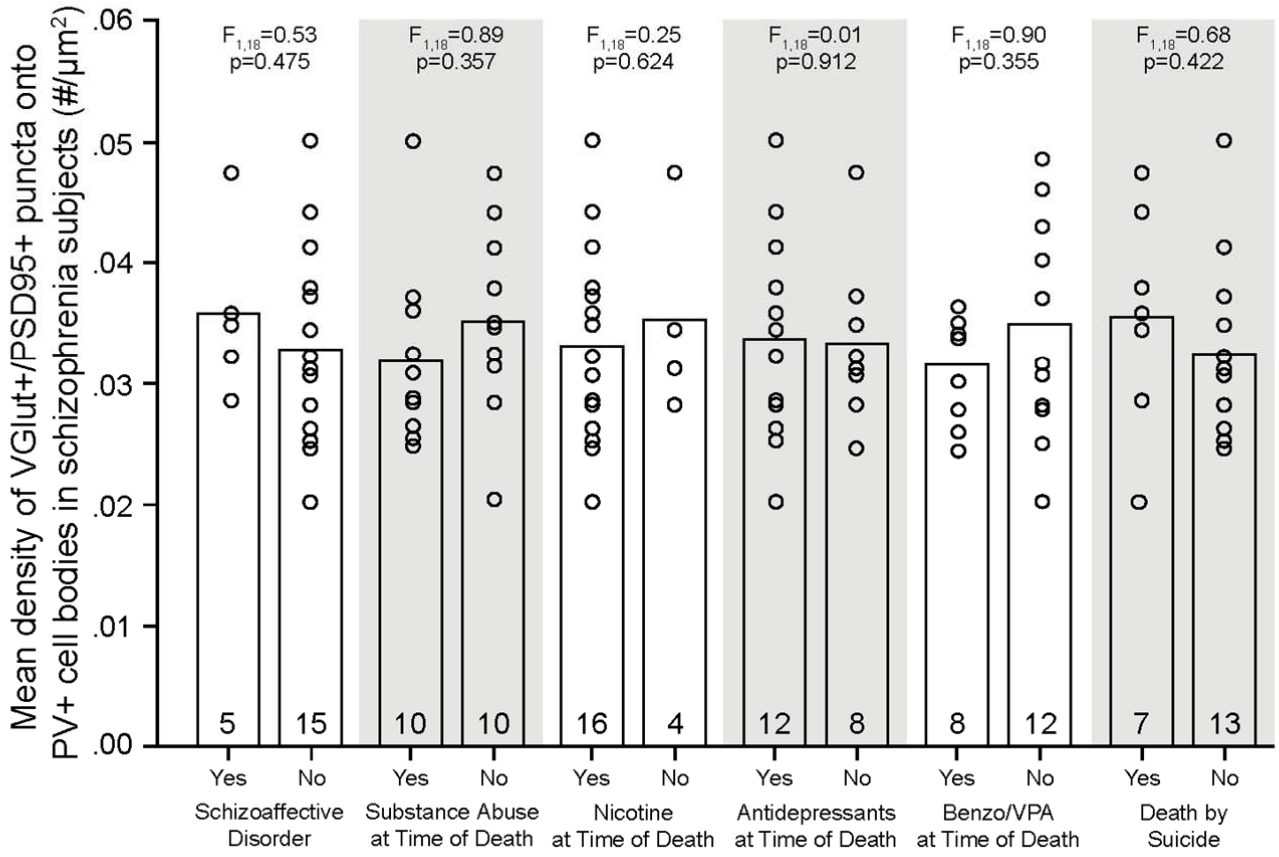

Supplementary Figure S4